Hybrid Genetic Algorithm and Kalman Filter Approach to Estimate the Clamping Force of Electro-Mechanical Brake

Junhyung Bae
Convergence Research Center for Future Automotive Technology, Daegu Gyeongbuk Institute of Science and Technology (DGIST), Daegu, Republic of Korea
baejunh@dgist.ac.kr

Sangjune Eum
Convergence Research Center for Future Automotive Technology, Daegu Gyeongbuk Institute of Science and Technology (DGIST), Daegu,Republic of Korea
sjeum@dgist.ac.kr

Seonghun Lee
Convergence Research Center for Future Automotive Technology, Daegu Gyeongbuk Institute of Science and Technology (DGIST), Daegu,Republic of Korea
shunlee@dgist.ac.kr

***Abstract*—In thispaper, a hybrid genetic algorithm (GA) and Kalman filter approach to combining motor encoder and current sensor models is presented to accurate estimate the clamping force of an electro-mechanical brake (EMB). Elimination of the clamping force sensor and measurement cables results in lower cost and increased reliability of an EMB system, including its electric motor.A Kalman filter is a special kind of observer that provides optimal filtering of the measurement noise and inside the system if the covariances of these noises are known. The proposed combined estimator is based on Kalman filter optimized by GA in which the motor encoder is used in a dynamic stiffness model and the motor current sensor is used to give measurement updates in a torque balance model. A real-coded GA is used to optimize the noise matrices and improve the performance of the Kalman filter. Experimental results show that, by using the proposed estimator, the virtual clamping force sensor can handle highly dynamic situations, making it suitable for possible use in sensorless fault-tolerant control. It is shown that the proposed combined estimator improves the root mean square error (RMSE) performance. The developed estimator can be used in real vehicle environments because it can adapt to parameter variations.**

***IndexTerms*—Electro-mechanical brake,Clamping force, Genetic algorithm, Kalman filter**

I. INTRODUCTION

Recently, X-by-wire (XBW) for vehicle electronic control has been actively studied in the automotive industry. XBW has the effect of improving the design freedom of the vehicle and the fuel efficiency by replacing existing mechanical hydraulics with electrical systems. It was developed to improve actuation response times by replacing the mechanically actuated systems used in conventional vehicles [1]. Furthermore, design and implementation of brake-by-wire (BBW) systems in the XBW has been the focus of researchers and industry experts for decades [2]. The human-machine interface (HMI) in the BBW system is provided by a pedal feel emulator. Such an electronic pedal is equipped with sensors that indicate the level of brake demand required by a driver. The output signals from these sensors are processed by an electronic control unit (ECU) that appropriately controls the actuators. A high level of safety is employed in BBW systems to ensure fault-tolerant operation.

The BBW systems approach reduces weight and is more environmentally friendly (due to brake fluid omission) than electro-hydraulic technologies. This scheme uses an electric motor drive coupled to a reduction gear set-up to provide brake control to each wheel. The BBW systems are divided into the electro-hydraulic brake (EHB) which electronically controls the hydraulic brake system using a solenoid valve, and the electro-mechanical brake (EMB) which controls the brakes directly using an electric motor. The EMB types can be divided into screw-type EMB with screw direct pressurization and electro-wedge brake (EWB) with self-reinforcement features of a wedge structure. The EMB system allows removal of the brake booster and hydraulic hose, so it requires less space, is eco-friendly, and provides faster response time. An electric motor coupled to reduction gearing is the general setup used for the EMB actuator. The motor is typically a three-phase permanent magnet synchronous motor (PMSM) or brushless DC motor for reasons of compactness and enhanced commutation efficiency. Moreover, there are no sparks in this case, unlike when using a brush-type motor. A planetary gear-set connected to a ball-screw are generally the components used in the reduction gearing. The reduction gearing generally consists of a planetary gear-train connected to a ball-screw that can generate clamping force.

To control the EMB caliper clamping force, a clamping force sensor is typically used to close the control loop. A standard motion control architecture (cascaded force, speed, and current control loops), after slight alteration, can be used to control an EMB. Line et al. [3] exchanged the position control loop with a force control loop for EMB control purposes. The control system requires the use of the force sensor (normally an encoder), and the current sensor for a three-phase PMSM.

A clamping force sensor is a relatively high-cost device. The elimination of a clamping force sensor from EMB designs is highly desirable because of the cost, engineering problems, and research challenges involved with its use. Moreover, if a clamping force sensor is placed close to a brake pad, it will

IRJECE

This is an open access article under the CC BY-SA 4.0 license (https://creativecommons.org/licenses/by-sa/4.0/)

then be subjected to severe high temperature that would challenge its mechanically integrity. This situation can be avoided by embedding a clamping force sensor deep within the EMB, (i.e. at the near end of the ball-screw). It has been shown that embedding a sensor in this way leads to hysteresis that is influenced by friction between the clamping force sensor and the pad and disk interface. This hysteresis significantly influences the accuracy of the clamping force measurement.

Due to the cost issues and engineering problems involved with using an actual clamping force sensor, an opportunity presents itself for the development of a virtual clamping force sensor. That is, the opportunity here is to accurately estimate the clamping force based on alternative sensor measurements, leading to omission of a clamping force sensor. Accurate clamping force estimation techniques are important for automotive safety-critical systems, and highly dynamic braking situations are known to cause significant inaccuracies in typical clamping force estimation. Also, if the EMB system fails to operate due to a sensor failure, the braking force is lost and the probability of a fatal accident rises sharply.

The focus of this work is to develop a virtual clamping force sensor for sensorless control of automotive BBW systems. Two independent models (dynamic stiffness model and torque balance model) were proposed to estimate clamping force with the help of information from the remaining sensors. Then, a hybrid approach using a genetic algorithm (GA) and Kalman filter was developed to improve clamping force estimation performance. The GA was applied because the distribution of noise is usually known, and manual tuning of the Kalman filter using the trial-and-error is very time consuming. A real-coded GA was used to optimize the noise matrices and thereby improve the performance of the Kalman filter. The dynamic stiffness model was used as the state-space system equation, and the torque balance model was used as the measurement equation.

II. THE EMB SYSTEM MODELING

In this chapter, we briefly summarize the EMB system. Figure 1 shows the configuration of the EMB which consists of an electric brake motor, ball-screw, caliper, brake pad, and disk.

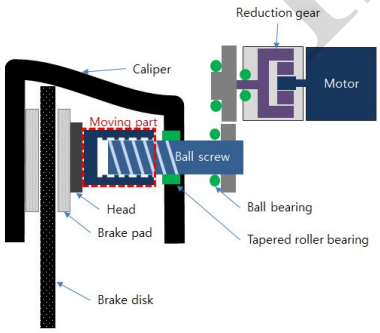

Fig 1. Configuration of the EMB

A. Electrical Modeling of the EMB

The EMB system is an electro-mechanical system consisting of an electric motor, caliper, and disk. Therefore, this system requires a complex modeling of both the electric motor (electrical part), and the caliper and disk (mechanical parts).

The motor torque and the motor speed, which correspond to output quantities of the electrical subsystem, are dependent on the controllable magnitude and the adjustable frequency of the inverter output currents, i_a, i_b, and i_c. The three-phase inverter output currents, produced by the pulse-width modulation of the three-phase inverter, are generally dealt with as the dq-axis currents i_d, i_q, and the neutral-axis current i_n in the electronic controller that performs the speed and torque control.

The dq transformation is used for PMSM to transform the reference frame of the voltage, current, and magnetic flux [4].

$$\begin{aligned} v_d &= Ri_d + \frac{d}{dt}\left(L_d i_d\right) - \omega_r \psi_q \\ v_q &= Ri_q + \frac{d}{dt}\left(L_q i_q\right) + \omega_r \psi_d \\ \psi_q &= L_q i_q, \psi_d = L_d i_d + \phi \end{aligned} \tag{1}$$

where v_d, v_q is the d-axis and q-axis voltage; i_d, i_q is the d-axis and q-axis stator current; R is the resistance; L_d, L_q is the d-axis and q-axis inductance; ψ_d, ψ_q is the d-axis and q-axis flux linkage; ω_r is the motor synchronous speed (or electrical angular speed); ϕ is the flux linkage due to magnetic rotor.

The electrical motor torque of the PMSM can be expressed as,

$$T_m = \frac{3}{2} P\left[\phi i_q + \left(L_d - L_q\right) i_d i_q\right] \tag{2}$$

The maximum torque is generated in the PMSM when the magnetic rotor and the rotating frame are maintained at a right angle with the three-phase current control. In this case, the d-axis current, i_d, is set to zero and the following assumption is made.

$$T_m = \frac{3}{2} P \phi i_q = k_m i_q \tag{3}$$

wherek_m is a motor torque constant. The relationship between the synchronous speed ω_r and the rotational speed ω_m is as follows.

$$\omega_m \approx \frac{1}{P} \omega_r \tag{4}$$

B. Mechanical Modeling of the EMB

The system used in this study is a method of generating the clamping force needed to push the brake pads. The torque generated by the motor is changed from rotational to translational motion through a ball-screw; then transmitted to the brake pad. The mechanical components of the model are expressed as,

$$T_m = T_l + J \frac{d}{dt} \omega_m + T_f \tag{5}$$

IRJECE

This is an open access article under the CC BY-SA 4.0 license (https://creativecommons.org/licenses/by-sa/4.0/)

where T_l is the load torque, J is the moment of inertia, ω_m is the motor angular speed, T_f is the resistance torque due to friction and viscosity.

The load torque is directly related to the clamping force between the brake pad and rotor. The resistance torque is mainly from viscous friction torque in the ball-screw.

$$T_l = \frac{p_s}{2\pi n_g \eta} F_{cl} = \gamma F_{cl} \tag{6}$$

whereF_{cl} is the clamping force, p_s is the screw pitch, n_g is the gear ratio, $\eta$is the screw efficiency, and γ is the gear-train gain.

C. Nonlinear Characteristics in the EMB

The dominant nonlinearities to consider in the EMB system are force ripple and friction. These are caused by the electromagnetic structure of the motor, the mechanical structure from which torque generated by the motor is converted to the clamping force through the caliper and other imperfect physical factors.

Force ripple is caused by cogging force and reluctance force. The cogging force occurs as a result of mutual attraction between the rotor magnet and the slot of the stator, which occurs even when no current flows through the windings and appears as a periodic relationship to the position of the stator relative to the magnet. The reluctance force is caused by the change in the self-inductance of the winding to the relative position between the magnet and the stator. In particular, the force ripple appears to be large at low speed or low load. In order to solve this problem, it is necessary to design the motor with consideration of the electromagnetic structure to minimize the force ripple, and to provide a control technique for ripple rejection.

Friction is the most nonlinear phenomenon in the entire system due to the nonlinear characteristics of all mechanical systems. This phenomenon is also seen in the EMB system, which causes errors and performance degradation.

Several models have been proposed to explain the phenomenon caused by friction. In general, friction acts in the direction opposite the motion, and the friction model is expressed in the form of a function of velocity. A typical friction torque model can be represented by a combination of Coulomb friction, viscous friction, and Stribeck friction torque [5].

$$T_f = \left[T_c + (T_s - T_c) e^{-|\omega_m/\omega_s|^2} \right] \mathrm{sgn}(\omega_m) + B_v \omega_m \tag{7}$$

where T_c is the Coulomb friction torque, T_s is the stiction friction torque, ω_s is the Stribeck velocity, and B_v is the coefficient of viscous friction.

III. ESTIMATION OF THE EMB CLAMPING FORCE

A. Dynamic Considerations

Figure 2 shows the clamping force versus motor angular position where the latter is varied in a uniform random manner. It is apparent from Figure 4 that there is significant dynamics in the system, and that the use of a characteristic curve to estimate the clamping force has limitations for highly dynamic cases. The clamping force was elevated during applying and reduced during the release. The cause of this dynamic will be described and modeled in the following section.

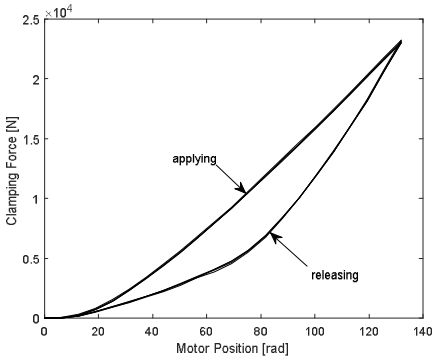

Fig 2. Characteristic curve of the EMB

B. Dynamic Stiffness and Torque Balance Modeling

To determine an induced clamping force in an EMB caliper using motor current information, the model can be solved as follows:

$$F_{cl} = \frac{k_m i_q - J \dfrac{d^2\theta_m}{dt^2} - T_f}{\gamma} \tag{8}$$

Application torque T_l is linearly proportional to the clamping force F_{cl} with reduction gearing gain γ, which is determined using the specifications from the gear-train and ball-screw. The inertial torque is linearly proportional to the motor angular acceleration $d^2\theta_m/dt^2$ with a lumped inertia gain J that involves both rotational and translational motions.

Eq. (8) shows that the frictional torque T_f term is undefined, this is because as Olsson et al. [5] explained, deriving an accurate friction model from first principles is simply not possible due to the random nature of friction. To improve accuracy, general friction models should be used in accordance with compensation for friction phenomena that occur in a particular system. Friction models of any sort tend to be avoided in trying to estimate the clamping force in an EMB caliper because of issues related to accounting for wear in the reduction gearing.

Employment of an applying and releasing action technique avoids the need for using a friction model, which is explained in more detail as follows [2]. At both these instants the application of Eq. (8) yields:

$$T_{m,cl} = \gamma F_{cl} + J \frac{d^2\theta_{m,cl}}{dt^2} + T_f$$
$$T_{m,rl} = \gamma F_{cl} + J \frac{d^2\theta_{m,rl}}{dt^2} - T_f \tag{9}$$

IRJECE

This is an open access article under the CC BY-SA 4.0 license (https://creativecommons.org/licenses/by-sa/4.0/)

where $T_{m,cl}$ and $T_{m,rl}$ indicate applying and releasing torque, respectively. The friction terms in Eq. (9) have approximately the same magnitudes but opposite signs due to the change in the course of motor travel. Adding Eq. (9) cancels out the friction terms, and after some manipulation the following equation to estimate clamping force F_{cl} can be found:

$$F_{cl} = \frac{T_{m,cl} + T_{m,rl} - J\dfrac{d^2\left(\theta_{m,cl} + \theta_{m,rl}\right)}{dt^2}}{2\gamma} \tag{10}$$

Saric et al. [6] developed a dynamic stiffness model to handle such viscoelastic effects. Consider a first order transfer function expressed by the following equation:

$$G(s) = \frac{F_{cl}(s)}{\theta_m(s)} = \frac{K_t}{\tau s + 1} \tag{11}$$

where θ_m and F_{cl} denote the motor angular position and estimated clamping force in s-domain, respectively. The gain K_t and time constant τ are the parameters to be determined. Converting Eq. (11) into time-domain yields:

$$F_{cl} = K_t\theta_m - \tau\frac{dF_{cl}}{dt} \tag{12}$$

When the electric motor is at low speed $dF_{cl}/dt \approx 0$, therefore the clamping force will nearly be linearly proportional to the motor angular position. However, as shown in Figure, a characteristic curve for an EMB is non-linear and can be accurately described by a third-order polynomial. This non-linearity, at the very least, can be attributed to variation in stiffness exhibited by the brake pads and the caliper bridge. Based on this, a more accurate variation of Eq. (12) is as follows:

$$F_{cl} = \Lambda_2\theta_m^3 + \Lambda_1\theta_m^2 + \Lambda_0\theta_m - \tau\frac{dF_{cl}}{dt} \tag{13}$$

where Λ_2, Λ_1, and Λ_0 are stiffness parameters. The discrete-time notation of Eq. (13) is more practical for use in a digital processing system and is expressed in a simplified form as follows:

$$F_{cl}(k) = \alpha_3\theta_m^3(k) + \alpha_2\theta_m^2(k) + \alpha_1\theta_m(k) + \alpha_0 F_{cl}(k-1) \tag{14}$$

where α_3, α_2, α_1, and α_0 are experimentally determined constants. Because high speed measurement was used for parameter tuning in Eq. (14) such situations are weighted more heavily with regards to accuracy. This is a desired outcome because it allows performance for high deceleration safety-critical braking situations to be optimized.

The following chapter details how we setup the novel Kalman filter optimized by GA for tracking EMB clamping force obtained from Eq. (10) and (14).

IV. DESIGN OF A HYBRID GA AND KALMAN FILTER TO COMBINE THE MODELS

A. Combining the Dynamic Stiffness Model and Torque Balance Model Using a Kalman filter

In the previous chapter, we introduce the dynamic stiffness model and the torque balance model. In this chapter, we design a Kalman filter suitable for the EMB clamping force virtual sensor and fuse and track both models. A Kalman filter is a linear, recursive, and optimal estimator and is widely implemented in control systems to give improved system state estimates.

The derivation of the Kalman filter algorithm is as follows. A discrete state-space representation of a linear dynamic system with noises may be written in the following form:

$$\begin{aligned} x(k) &= Ax(k-1) + Bu(k) + w(k-1) \\ z(k) &= Hx(k) + v(k) \end{aligned} \tag{15}$$

where x is the system state vector, u is the control inputs, w is the process error vector, z is the measurement vector, v is the measurement error vector, K is the Kalman filter gain, A is the transition matrix, B is the control input matrix, and H is the measurement matrix.

It is assumed that the transition matrix and control input matrix are not time-varying. The discrete-time notation, $k|k-1$, indicates that the estimate at k was determined given knowledge at $k-1$. The linear estimator and filter gain are defined as follows:

$$\hat{x}(k|k) = \hat{x}(k|k-1) + K(k)\left[z(k) - H\hat{x}(k|k-1)\right] \tag{16}$$

$$K(k) = P(k|k-1)H^T(k)\left(H(k)P(k|k-1)H^T(k) + R\right)^{-1} \tag{17}$$

where P is the covariance matrix of state estimates, and R is the measurement error covariance matrix.

The matrices $P(k|k-1)$ and $P(k|k)$ for a Kalman filter are given below as:

$$P(k|k-1) = A(k)P(k-1|k-1)A(k)^T + Q \tag{18}$$

$$P(k|k) = \left(I - K(k)H(k)\right)P(k|k-1) \tag{19}$$

where Q is the process error covariance matrix, and I is the identity matrix.

It should be noted that the process error covariance Q and measurement error covariance R matrices may be time-variant, however, here; we assume them to be constant. A Kalman filter of any type involves the recursive application of prediction and filtering cycles.

To employ a Kalman filter for the EMB clamping force estimation, we first used Eq. (14) as our state-space system equation. The constant α_0 from Eq. (14) is taken to be equal to $A(k)$. The clamping force in Eq. (14) is non-linearly proportional to the motor position input data. This non-linearity does not require the use of an extended Kalman filter (EKF)

IRJECE

This is an open access article under the CC BY-SA 4.0 license (https://creativecommons.org/licenses/by-sa/4.0/)

because it is not state dependent. To integrate this non-linearity within the Kalman filter we apply the following equality:

$$A(k)x(k-1) = \alpha_0 F_{cl}(k-1), \quad B(k)u(k) = \alpha_3\theta_m^3(k) + \alpha_2\theta_m^2(k) + \alpha_1\theta_m(k) \tag{20}$$

where $\hat{x}$ is taken to be $\hat{F}_{cl}$. The a priori estimate of the state $\hat{F}_{cl}(k|k-1)$ is taken to be directly equal to $\hat{z}(k|k-1)$. The measurement equation is as follows:

$$\hat{z}(k|k-1) = \hat{F}_{cl}(k|k-1), \quad z(k) = F_{cl}(k) + v(k) \tag{21}$$

For this situation, the matrix $H(k)$ is taken to have a constant unit value. In Eq. (21), the measured data is substituted into the calculated clamping force of Eq. (10). The two models are combined using the Kalman filter to give an optimized estimate of clamping force. Figure shows a block diagram of the Kalman filter applied to the EMB system.

B. Optimizing the Noise Matrices of a Hybrid Genetic Algorithm and Kalman Filter

Since we cannot know Q and R matrices in a real vehicle environment, we propose a method to improve the EMB clamping force estimation performance by applying optimization technique to the Kalman filter.

The GA has a powerful encoding mechanism that enables the representation of a solution vector as either a binary string or real-coded. In order to find the best matrices Q and R for the Kalman filter, a real-coded GA was employed. The real-coded GA has many advantages for optimization of numerical function over binary encoding. Efficiency of the real-coded GA is increased because there is no need to convert chromosomes to phenotypes before each fitness evaluation; less memory is required and; there is no loss in precision from the conversion between binary and real values. The procedure for making the real-coded is outlined as follows:

1. Population Representation: The covariance matrices Q and R are coded into a long real-coded string, chromosome.
2. Initial Generation: The process begins by randomly generating an initial population of long real-coded strings.
3. Fitness Evaluation: In the current generation, each of the strings is decoded back to the corresponding diagonal elements of the two matrices. Then, these diagonal elements from each string are separately sent to the Kalman filter of the EMB system to yield an objective function. Finally, these strings are ranked according to the value of the objective function by a linear ranking method.
4. Reproduction: Reproduction is a process in which parent structures are selected to form new offspring (children). For this, the stochastic universal sampling method was employed.
5. Crossover: The single-point recombination method is used to exchange information between two chromosomes.
6. Mutation: A breeder GA is used to implement the mutation operator for the real-coded GA, which uses a nonlinear term for the distribution of the range of mutation applied to the gene values.
7. Replace: Place new offspring in the old population to create a new population and use the newly generated population for the next run of the algorithm.
8. Iteration: The real-coded GA runs iteratively repeating processes 3) to 7) until a population convergence condition is met, or the given maximum number of iterations is reached.

The proposed concept of clamping force estimation is shown in the following Figure 3.

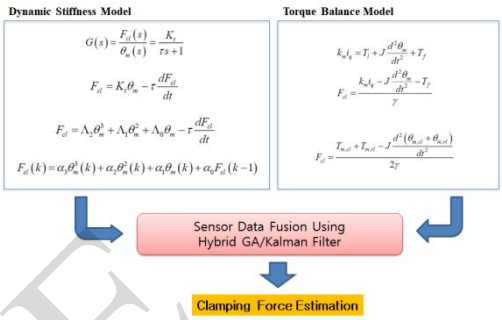

Fig 3. Proposed concept of clamping force estimation

V. EXPERIMENTAL SETUP AND RESULTS

A. Experimental Setup

Our test bench was setup for use on the newly developed EMB caliper. Figure 4 shows the developed systems. The electric motor is of the PMSM-type maxon EC-4 pole 30 motor, with ratings of 200 W and 15,000 rpm and ensures that maximum clamping forces can be achieved. To interface with the motor and ECU devices, the CAN and FlexRay networks were utilized. The PC provides a real-time operating system that was implemented to control the motor position. The electric motor is controlled by cascaded PI controller with the standard motion control architecture; force, speed, and current control loops.

The PC has an Intel Core CPU 1.5 GHz and RAM 8 GHz. To measure the motor position, encoder output is taken from the coupled the servo-motor. The resolution of this encoder output provides 1,000 counts per turn. A clamping force sensor is placed in between the brake pads to measure the actual force induced by the brake pads. The sensor data was collected using the DEWETRON monitoring system. The monitoring system updates in-vehicle information received from each ECU via CAN and overall EMB status information in real-time. Figure 5 shows the actual clamping force signal measured for 32 seconds for the stepwise dynamic braking. The clamping force sensor data was gathered at 0.2 ms sample intervals. Therefore, total acquired data are 160,000 samples.

IRJECE

This is an open access article under the CC BY-SA 4.0 license (https://creativecommons.org/licenses/by-sa/4.0/)

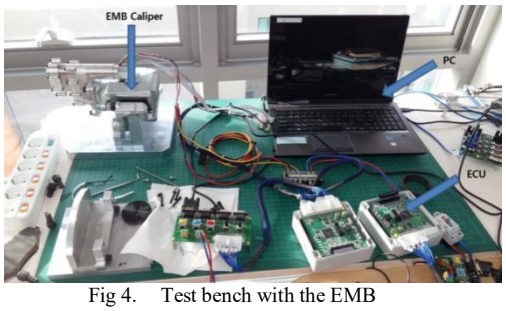

Fig 4. Test bench with the EMB

B. Comparison of Results and Discussions

The Kalman filter used for tracking the clamping force was applied to the two model's data. We used constant process error variance of 1 and measurement noise variance of 1 to initialize the error variance. Then, the GA was implemented on the PC. To optimize the noise matrices of the Kalman filter for the EMB system, the parameters of the GA were set as follows:

- Initial population size: 40,
- Maximum number of generations: 20,
- Probability of crossover: 0.9,
- Mutation probability: 0.01,
- Initial range of real-coded strings: [0.0001; 0.1].

Figure 5 shows the estimation performance of the proposed method to track the clamping force in the EMB system for various clamping force. We used the root mean squared error (RMSE) between actual and estimated values as performance indicators. During total 32 seconds, RMSE of the dynamic stiffness model and torque balance model was 404.670 N and 413.773 N, respectively. The RMSE of the hybrid GA/Kalman filter was 324.796 N. This is approximately 21.44% improvement on the RMSE of the Kalman filter alone of 413.449 N for total 32 seconds. Therefore, we have demonstrated that the use of hybrid GA/Kalman filter which has a recursive aspect, improves the RMSE performance of the clamping force estimation.

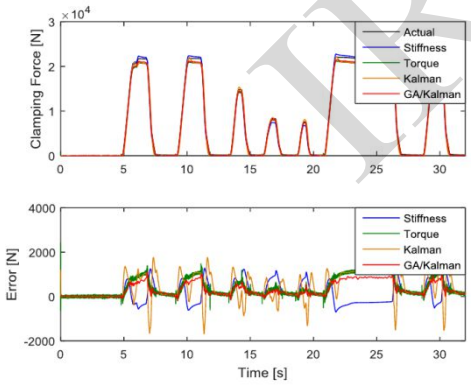

Fig 5. Estimation results

VI. CONCLUSIONS

In this paper, we proposed a cost and design effective solution for an automotive EMB actuator in BBW systems. The objective of making a virtual clamping force sensor in the EMB system is strongly encouraged by the results. A dynamic stiffness model was used to estimate the clamping force that relied on output from an encoder. Based on a torque balance approach, a second model was used to estimate the clamping force that relied on the use of the motor current sensor and encoder. The outputs from the two independent models were combined using a hybrid GA/Kalman filter to give accurately track the actual clamping force.

The newly developed estimator was shown via experimental verification to be able to handle highly dynamic braking situations. Real-coded GA was found to be a power technique for optimizing the Kalman filter as applied to the EMB system. Based on a real-coded GA, the optimization procedure enables the noise matrices, on which the Kalman filter performance critically depends, to be properly selected.

The experimental results demonstrated that the Kalman filter optimized by GA has good noise rejection and that its performance is less sensitive during the dynamic braking. With continued development, the possible cost savings inherent in making an accurate virtual clamping force sensor could be accomplished in the EMB implementations. However, the clamping force estimator validations were not performed yet on a rotating disk in the real car. The significance of this issue should be investigated in future work.

ACKNOWLEDGMENT

This work was supported by the DGIST R&D Program of the Ministry of Science and ICT (17-IT-01).

REFERENCES

[1] R. Schwarz, R. Isermann, J. Böhm, J. Nell, and P. Rieth, "Modeling and Control of an Electromechanical Disk Brake," SAE Tech. Paper 980600, 1998.

[2] Y. H., Ki, and H. S. Ahn, "Fault-Tolerant Control of EMB Systems," SAE Tech. Paper 2012-01-1795, 2012.

[3] C. Line, C. Manzie, and M. Good, "Control of an Electromechanical Brake for Automotive Brake-By-Wire Systems with an Adapted Motion Control Architecture," SAE Tech. Paper 2004-01-2050, 2004.

[4] W. Hwang, K. Han, K. Huh, J. Jung, and M. Kim, "Model-based Sensor Fault Detection Algorithm Design for Electro-Mechanical Brake," 14th Int. IEEE Conf. on Intelligent Transportation Systems, Washington, DC, USA, Oct. 2011.

[5] H. Olsson, K. J. Åström, C. Canudas de Wit, M. Gäfvert, and P. Lischinsky, "Friction models and friction compensation," European Journal of Control, 4(3), pp. 176-195, 1998.

[6] S. Saric, and A. Bab-Hadiashar, "Clamp Force Estimation for a Brake-By-Wire System: A Sensor Fusion Approach," IEEE Trans. on Vehicular Technology, vol. 57, no. 2, pp. 778-786, Mar. 2008.

IRJECE

This is an open access article under the CC BY-SA 4.0 license (https://creativecommons.org/licenses/by-sa/4.0/)